Sub-coil in reader antenna for HF RFID volume detection improvment

Marjorie Grzeskowiak, Megdouda Benamara, Patrick Poulichet, Stéphane Protat, Gaëlle Lissorgues, Antoine Diet, Marc Biancheri-Astier, Yann Le Bihan, Christophe Conessa, Francisco de Oliveira Alves

Sub-coil in reader antenna for HF RFID volume detection improvment

M.Grzeskowiak, M.Benamara, P.Poulichet, P.Protat
G.Lissorgues
ESYCOM EA 2552
(UPEMLV, ESIEE-Paris, CNAM)
Cite Descartes, F. 77454 Marne-la-Vallée, France
Cite Descartes, BP99, 93162 Noisy le Grand
marjorie.grzeskowiak-lucas@u-pem.fr

A. Diet, M. Biancheri-Astier,
Y. Le Bihan, C. Conessa, F. Alves
GEEPs UMR 8507, Univ. Paris Saclay
(CNRS, CentraleSupélec, Univ. Paris-Sud, UPMC)
11, rue Joliot Curie, Plateau de Moulon,
F 91192 Gif-sur-Yvette, France

***Abstract*—This paper proposes a reader antenna, improving the inductive coupling with a small coil whatever its position or orientation against the reader antenna. Sub-coils are inserted and the turn number is optimized in order to improve efficiency of the inductive coupling in the case of HF RFID volume detection in keeping constant the magnetic energy generated by the reader.**

Keywords—HF RFID; Distributed Diameter Coil; Twisted Loop Antenna; off-center subcoils; volume detection; read range improvement

I. INTRODUCTION

In 13.56 MHz RFID (Radio Frequency IDentification) or in inductive WPT (Wireless Power Transfer), the received power is affected by the distance and by the angular misalignment between the coils. Futhermore, greater the size ratio between the coils is, weaker is the received power. In the case of RFID, the reader input impedance depends on the magnetic coupling and on the induced field in the transponder [1]. Although, stronger magnetic coupling could result in frequency shift: the transponder could be not detected. The objectives will be to improve the magnitude of the reader input impedance in minimizing its phase shift.

In this study, sub-coils [2] in complementary coils [3] are combined to improve the RFID detection for a small tag (in comparison with the size of the reader coil). The complementary coils allow detection of a tag placed perpendicularly to the reader plane (defined as VM mode), not only on the edges of the loop but also in the center of the structure. The sub-coils increase the magnetic coupling when the tag surface and this of the reader surface are parallel (HM mode) and perpendicular. Preliminary studies on coaxially sub-coil in complementary coils were done in [4]: RFID read-out distance at one point verify the improvement of the sub-coil structure for both orientations of the tag, but the magnetic coupling is weaker in the case of VM mode. In order to optimize the detection volume whatever tag's orientation, weaker magnetic coupling in VM mode has to been improved.

In the following section, the components of the magnetic field generated by the reader are carried out using magneto-statics module Radia [5]. The coupling coeffcient is calculated for both orientations of tag versus the misalignment on the (y) axis firstly for each radius of coils. Then the current of sub-coils is modified and its impact on the maximum mutual inductance is reported versus the reader inductance with electromagnetic software [6]. The better structures, in terms of mutual inductance and defined Figure Of Merit, are selected and compared with a quantified parameter, as input reader impedance: the reader inductances are around the same order to generate comparable magnetic energy. RFID volume detection is illustrated via detection cartographies for selected structure in both orientations of the tag.

II. OFF CENTER TWISTED LOOP ANTENNA

A. Contexte

In the case of RFID, the volume to prospect could be wide in comparison with the object to detect. This latter one could be oriented arbitrary and can be displaced; for instance, tagged pebbles [7] with a movable reader coil on sea-beach, clinical patient in a hospital [8] or surgeon devices sliding in an inclined tube [9]. A solution could be to design a planar transmitting antenna that generates magnetic field with the same intensity over the entire surface of the reader antenna but several orientations versus the zone of the reader antenna. The mutual inductance with the received antenna will be increased on a large area in both orientations, when the transponders are perpendicularly and parallel to the plane of the transmitting antenna, that can be useful to receive power when the transponder is oriented to 45°degrees from the planar transmitting antenna. First, the objective is to increase the magnetic coupling in the worst case, i.e. when the transponder is perpendicular to the reader surface and then to optimize the geometrical coil in the best case, i.e. when the transponder surface is placed parallel to this of the reader one.

Complementary coils [3] increase magnetic coupling in the intersection of the coils when the transponder is perpendicular to the reader surface (VM mode in Fig.1.b) and Distributed Diameter Coil [4] allows especially the detection in HM mode, i.e. when the transponder is placed parallel (Fig.1.a). The figures 1.a and 1.b represent respectively the coils system in HM and VM modes with the (0xyz) coordinates system.

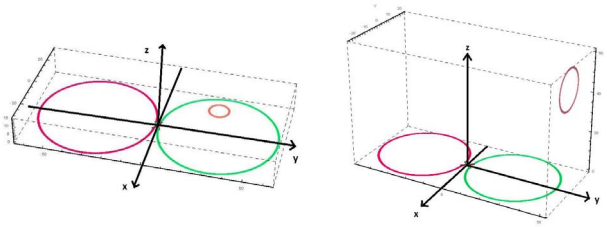

a) in HM modes b) in VM modes

Fig.1. Simulated coils systems in HM and VM modes

In the following part, the magnetic induction in calculated for each component, and its integration on the receiving coil allows evaluating the inductive coupling.

B. Optimization of coil radius

The magnetic induction generated by the transmitting coil (Fig.2 and Fig.3), and the mutual inductance with a receiving coil (Fig.4) are carried out using magneto-statics module Radia [5]. The receiving coil is one-turn coil of 1cm diameter. The transmitting coil is simulated in considering firstly the connection between the complementary coils.

In the perpendicular direction away from the coil (integration of B-field around the whole circular receiving coil for HM mode), the maximum magnetic induction appears in the center of the sub-coils ($B_x = 0; B_y = 0; B_z = \max$) : at 10mm away from the transmitting coil, the maximum of B-field is obtained in the center of the complementary coils and is higher with the smallest value of radius.

In the parallel direction away from the coil ((x) and (y) axis), the maxima appear for the center of the structure ($B_x = max; B_y = max; B_z = 0$). Although, the (xOz) plane is a symmetry plane for the current distribution, so the magnetic induction $\vec{B}$ would be perpendicular to this plane and $\vec{B}$ belongs to the anti-symmetry (y0z) plane: B_x would be null on the (y) axis, and especially in the center of the structure, while it is not the case on the Fig.2.

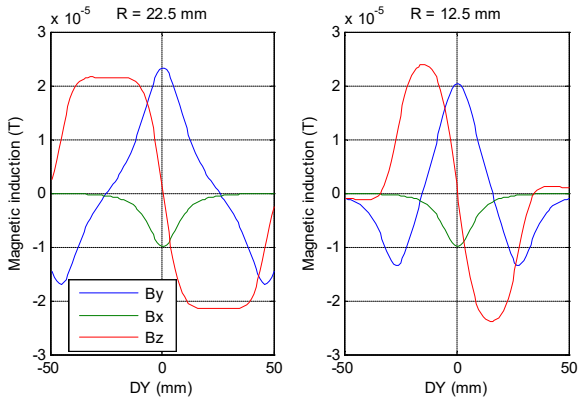

Fig.2 Simulated magnetic induction versus (y) misalignment at 1 cm for radius R of 22.5mm and 12.5mm

To explain the origin of B_x, the connection between the complementary sub-coils is removed in keeping the current flow direction as previously (Fig.1.b). In this case, for R=22.5mm, x-component of B-field B_x is 10^6 times smaller than this y-component B_y and can be considered negligible. The observation of the B-field generating by the transmitting coil with and without the receiving coil (Fig.3) allows seeing its disturbance on B-field. The greater modification appears for the y-component: the connection decreases the level of the B-field in the center of the structure with and without the receiving coil (comparison for DY=0 mm in Fig.2). Furthermore, in presence of the receiving coil, this component is completely modified: the value is superior above the exterior edge of the structure.

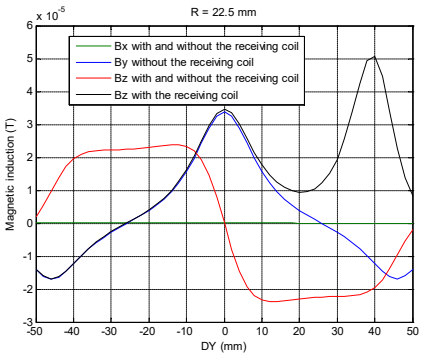

Fig.3 Simulated magnetic induction versus (y) misalignment at 1 cm for radius R of 22.5mm with and without the receiving coil

To observe the impact of the B-field on the received power, the coupling coefficient between the transmitting and receiving coils is calculated in Fig.4 with the connection and the presence of the receiving coil.

For the HM mode, the inductive coupling is better for the smallest coil while the available area is greater for the widest coil, as seen for the B-field (Fig.2).

In the case of VM mode, corresponding to the integration of the B-field y component B_y, the received power can be decreased due to the integration of the B-field x-component B_x and the B-field disturbance caused by the receiving coil: the maximum doesn't appear in the center of the structure but above the edge of the coils.

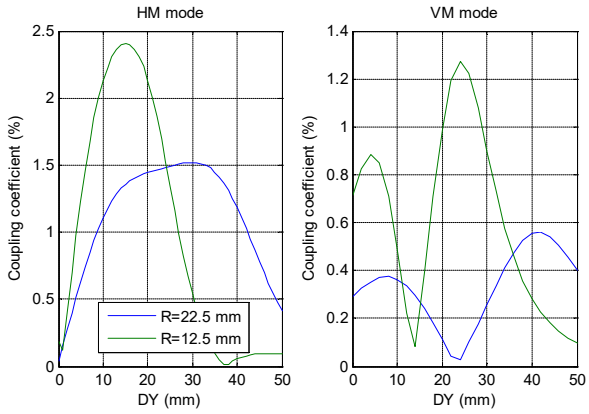

Fig.4 Simulated coupling coefficient versus (y) misalignment at 10cm for radius R of 22.5mm and 12.5mm in HM and VM modes

The impact of two radii for the complementary coils on the previous parameter confirms the interest to use these two radii in terms of level of coupling and available area in HM mode. The current can be modified to modify the distribution and orientation of B-field in order to maximize the received power. In VM mode, the disturbance of the B-field in the center of the structure (due to connection and presence of the receiving coil) could cause probably less enhancement as expected.

C. *Optimisation of coil current*

The following simulations were made with the help of full wave electromagnetic field simulator HFSS (High Frequency Structure Simulator) [6] to take into account the time variation, and its impact on the current distribution and on the B-field generation. The current is changed by modifying the turn number of each sub-coil. For the transmitting coil, the external diameters d_1 and d_2 of each sub-coil are respectively set to 4.5 cm and 2.5 cm, for instance, conventional 400 corresponding to ($4d_1$-$0d_2$), which 4 is the number of turn of the associated diameter d_1. A 1-turn loop receiving coil is used in simulation to reduce the computing time. The metalized part of the coils was substituted with infinite perfect electric conducting plane (PEC). The coils were supplied with the power of 1W.

The simulated maximum mutual inductance is obtained at 10 mm in HM mode (receiving coil parallel to the plane of the transmitting coil) when the coils are coaxial and in VM mode (receiving coil perpendicular to the plane of the transmitting coil) when the receiving coil is oriented perpendicularly in the center of the TLA structure. The disturbance of B-field caused by the connection and the presence of the receiving coil isn't observed in this case (Fig.2 and 3). Fig. 5 shows the simulated maximum mutual inductance versus the inductance of the transmitting coil for both VM and HM modes.

With 2µH self-inductance of the transmitting coil, the mutual inductance is higher in HM mode than in VM mode, while around 3µH, the VM mode is better than the HM mode.

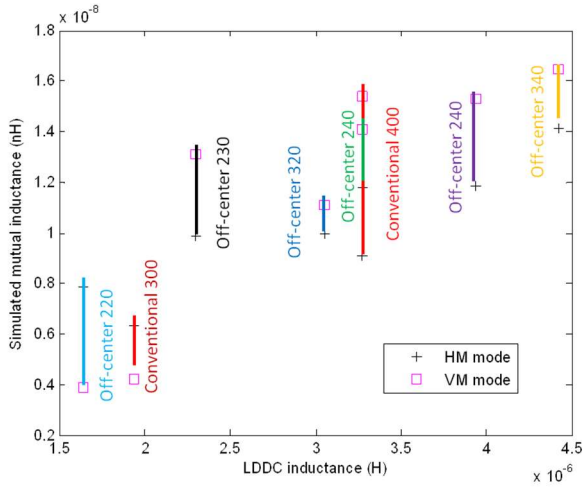

Fig.5 Simulated mutual inductance M(nH) versus the reader inductance LDDC(µH) in HM and VM mode at 1 cm

The off-center 240 structure that favors the using of 12,5mm radius seems more efficient in HM mode for self-inductance around 3.3µH, as suggested in Fig.2, in comparison with the conventional 400 and off-center 320. The same enhancement for HM mode appears for the off-center 220 against the conventional 300 coil.

To quantify the ability of coupling with a small coil, several parameters are calculated, like previously M (Mutual inductance), and CC (Coupling Capability) between transmitting and receiving coils. M and CC (1) can be used to optimize the wireless power transfer for best performances and have been identified for enhancement of reading distance for the inductive system and extension of the range of active area of the system (on DY axis in Fig.5), respectively. In order to normalize FoM(2), the maximum value M_{max} of M and inductance L_{DDC} of the DDC TLA are mixed with CC.

$$CC = \int_{Y_1}^{Y_2} |M(y)| dy \quad (1)$$

$$FoM = \frac{M_{max} \times CC}{L_{DDC}} \quad (2)$$

FoM can be varied by fluctuating the following parameters: sub-coil numbers of turns (Ni) and diameters of sub-coils (di). FoM is calculated for the structures in Fig.6. FoM is reported in HM and VM modes versus the simulated self-inductance (Fig.6) when moving according the receiving coil to dY (from 0 to 100mm with 2 mm step) at a distance DZ of 1 cm.

FoM is better for VM mode except for the conventional 400, while the mutual inductance is maximum for HM mode for reader inductance superior to 2µH.

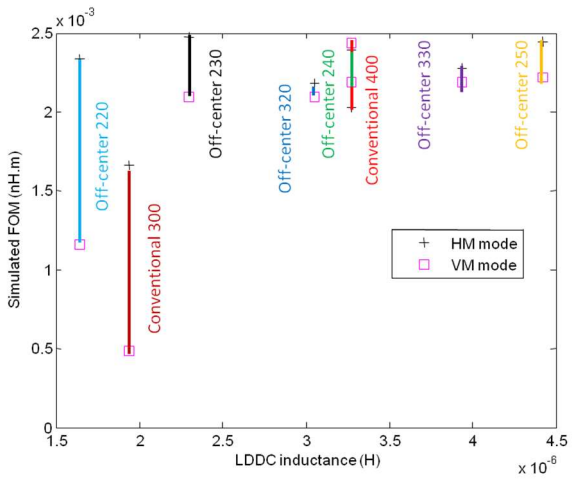

Fig. 6 Simulated figure of merit versus the inductance of the transmitting coil in VM and HM modes

In the following part, the off-center 240 is compared with the conventional 400: the mutual inductance and FoM are better for the off-center 240 in HM mode.

III. ELECTRICAL CIRCUIT AND READER INPUT IMPEDANCE

A. *Electrical model*

In order to observe the impact on the RFID detection, an electrical model is associated to the coils system and the reader impedance input Z_{in} allows quantifying the RFID detection; higher is the magnitude of the impedance input and weaker the

phase shift, better will be the detection of the transponder. These simulations are carried out using HFSS: the impedance of the reader (Z_{11}) is reported versus frequency firstly to fix the lumped electrical element and so the quality factor of the reader and then to observe the phase shift of the input impedance of the reader (Z_{in}).

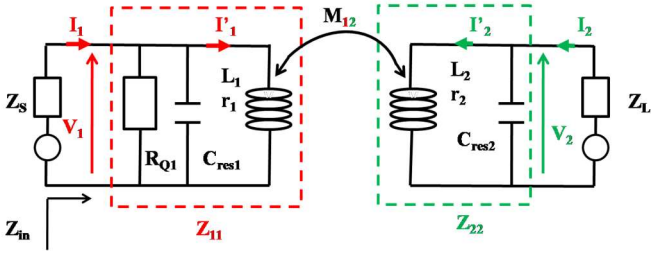

Fig.7. Electrical circuit

As seen in Fig.7, the input voltage V_1 and the output voltage $V_2$are given from currents I_1, I_1' , I_2 , I_2' and from the trans-impedance Z_{12} , the impedance of port 1 Z_{11}, this one of port 2 Z_{22} and the load impedance Z_L.

$$V_1 = Z_{11}I_1 + j\omega M_{12}I_2' = Z_{11}I_1 + Z_{12}I_2 \quad (3)$$

$$V_2 = -Z_L I_2 = Z_{22}I_2 + j\omega M_{12}I_1' = Z_{22}I_2 + Z_{21}I_1$$

The input impedance of the reader can be deducted as:

$$Z_{in} = Z_{11} + \frac{Z_{12}Z_{21}}{Z_{22}+Z_L} \quad (4)$$

with

$$Z_{11} = R_{Q1}//C_{res1}\,//(r_1 + j\omega L_1)$$

$$Z_{22} = C_{res2}\,//(r_2 + j\omega L_2)$$

$$Z_{12} = j\omega M_{12}\alpha$$

$$Z_{21} = j\omega M_{12}\beta$$

α and β parameters were calculated by the current divider bridge:

$$\alpha = \frac{I_1'}{I_1} = \frac{\left(Z_{R_{Q1}} + Z_{C_{res1}}\right)}{(r_1 + j\omega L_1) + \left(Z_{R_{Q1}} + Z_{C_{res1}}\right)}$$

$$\beta = \frac{I_2'}{I_2} = \frac{Z_{C_{res2}}}{(r_2 + j\omega L_{12}) + Z_{C_{res2}}}$$

Z_L is the load impedance and corresponds to the chip impedance in the case of RFID

The impedance matrix $\begin{bmatrix} Z_{11}Z_{12} \\ Z_{21}Z_{22} \end{bmatrix}$ is extracted directly from electromagnetic simulation with HFSS (High Frequency Structure Simulator) without determination of I_1' and I_2'.

To better sensitivity, the variation of input impedance from the impedance of port 1 $delta(Z_{in})$ (5) is calculated and reported versus misalignment at 1cm distance.

$$delta(Z_{in}) = Z_{in} - Z_{11} = \frac{Z_{12}Z_{21}}{Z_{22}+Z_L} \quad (5)$$

B. Simulated electrical model of the reader coil

On the tag side, resonance results from the parallel combination of capacitance of the chip C_L and the tag coil inductor L_2. In simulation, the diameter of 1-turn tag coil is 1cm and the electrical model corresponds to a resistance r_2 of 0.31 Ω and L_2 of 0.031µH; a parallel capacitance of 3.7nF is added and a quality factor of 10 is obtained (6).

$$Q = \frac{f_r}{f_2 - f_1} = \frac{13.50\times10^6}{(14.22-12.87)10^6} = 10 \quad (6)$$

The quality factor is no greater than 30 for the reader coil in order to have enough bandwidth for communication. Q_1 is reported in table 1 for the 400 conventional coil and off-center 240 structures, after parallel R_1 resistance and C_1 capacitance added to the reader coils.

TABLE I. ELECTRICAL MODEL OF READER COIL

Reader coil					
Name	$L_1(\mu H)$	$r_1(\Omega)$	$C_1(pF)$	$R_1(k\Omega)$	Q_1
400	3.27	3.17	41	10	26.4
240	3.27	2.81	42	9	27.2

In the following part, in the (y0z) plane (Fig.1), H-field is displayed for each selected structure with the same color scale.

C. Display of H-field

In the near field zone (Fig.8), the impact of the sub-coil can be seen clearly for the distribution and orientation of the magnetic field: the zone where the field is high is wider for the off-center structures and the orientation is more diverse.

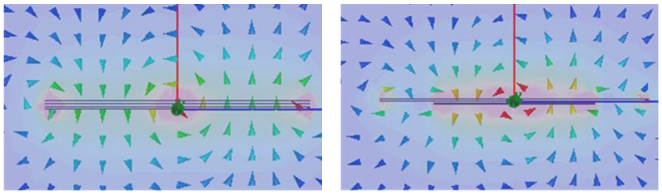

a) 400 b) 240

Fig.8. H-field display in (y0z) plane with same colour scale

The input impedance of the reader versus the transponder's displacement is reported for each structure.

D. Simulated imput impedance versus misalignment

The magnitude and phase of delta input impedance is reported versus the DY misalignment of the transponder in HM mode (Fig.9).

In HM mode, the phase of $delta(Z_{in})$ is around 165 degrees with variation of ±10 degrees. The variation of its magnitude is greater with the off-center 240 structure but the available area is smaller in this case.

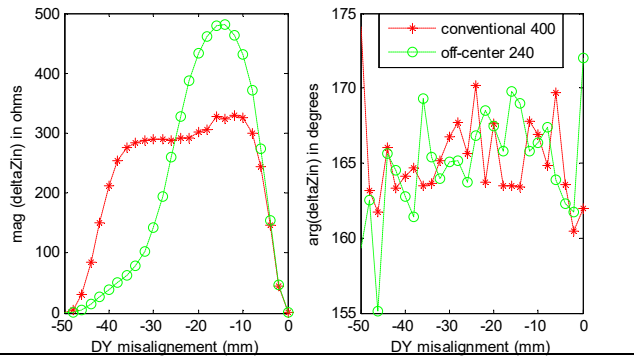

Fig.9. Reader impedance $delta(Z_{in})$ versus the misalignement of the tag at 10mm distance in HM mode

The structures are fabricated and 3D RFID detection realized to illustrate the improvement with the off-center 240.

IV. OFF CENTER RFID DETECTION

The diameters are set in the fabricated 3-D printing base, represented in figure 10. The enameled copper wire is rolled in the slots of the fabricated plastic base. Two combinations of turns with diameters in centimeter d_1 and d_2 are realized. The inductances of the sub-coils structure are measured with VNA and are respectively equal to 4.6µH and 4.8µH for the conventional 400 and the off-center 240. Parallel capacitance and resistance are added to obtain a 13.56MHz resonant frequency and the same quality factor.

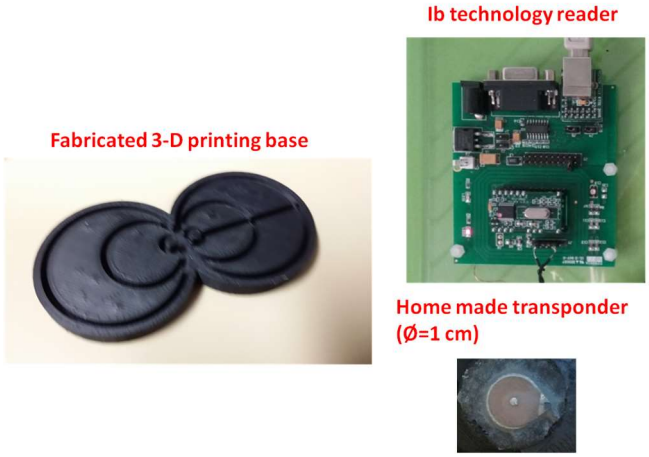

Fig.10. Photography of the fabricated 3D printing base, with Ib technology [10] and RFID home-made transponder.

The experimental test of increasing detection volume and surface is depicted in Fig.11 with sub-coils structure associated with Ib Technology UK [10].The RFID transponder is a spiral coil made by micro-etching (strip of 110 µm, inter-spire of 110 µm and 20 turns of 1cm diameter) on both side of the FR4 substrate.

The figure 11 is respectively the 2D plots of tag detection in HM mode with 400 conventional (a) and with off-center 240 (b). The (DY, DX) axes correspond respectively to a lateral misalignment according to the width and the length of the surface comprising the structures, the color scale defined the distance of detection DZ in mm.

As expected in Fig.9, the surface where the read-out distances is more important with the off-center 240. Although, the volume of detection is better for the conventional 400. The field generated by the enameled wire is too weak to be detected when the turn number is equal and inferior to 2: these structures would be realized with copper strip to reduce losses.

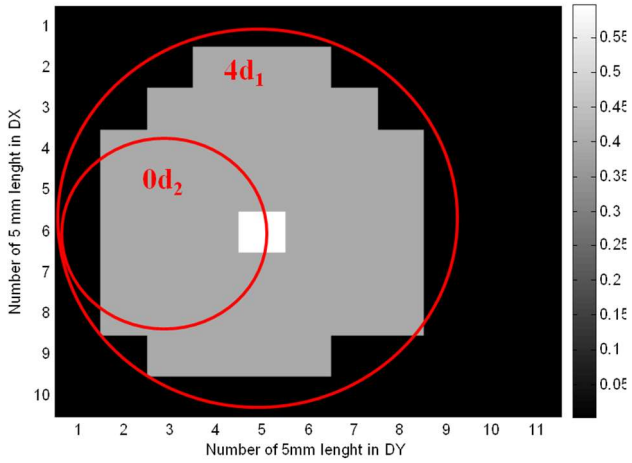

a) conventional 400

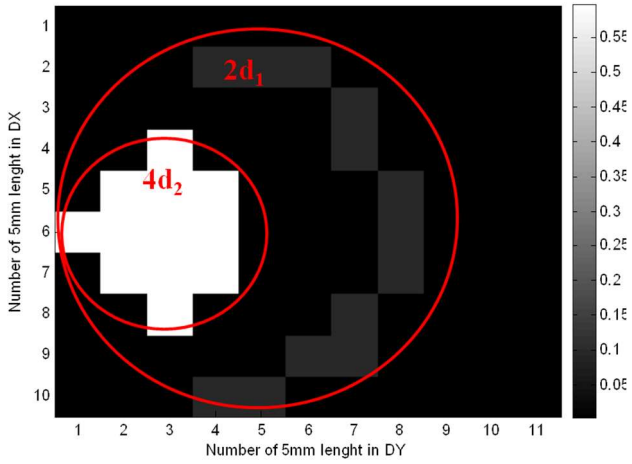

b) off-center 240

Fig.11. Surface and distance of detection in HM with conventional 400 (a), and with off-center 240 (b)

The detection in VM mode appears just in the center of the structure away 0.2mm from the structure: the hypothesis is that the connection between the complementary sub-coils degrades the magnetic induction, as seen in Fig.2 and that the presence of the receiving coil disrupt the B-field lines, as observed in Fig.3.

V. CONCLUSION

Sub-coil in reader coil allows changing distribution and

orientation of the magnetic induction. The objective with this design is to enhance the maximum coupling factor with a small receiving coil with an average coupling capability over a larger area. Magneto-static and magneto-dynamic softwares were used respectively to observe the magnetic induction and to calculate the input impedance of the reader in magnitude and phase. Numerical and experimental results show that the RFID distance read-out is improved, while the RFID detection area isn't as expected, due to wire losses and connection between sub-coils. Future work will focus on the realization of the sub-coil structures by micro-etching insertion to reduce wire losses: the connection that disrupts the magnetic induction and the detection in perpendicular orientation of the transponder has to be optimized.

ACKNOWLEDGMENT

This research funded by Paris-Est University was conducted by M. Grzeskowiak over a six-month visiting period in Paris Electrical and Electronic Engineering *Laboratory* (*GeePs*) at Paris-Sud University.

REFERENCES

[1] K.Finkenseller, "RFID Handbook: Radio-frequency Identification fundamentals and application", 2nd edition, Wiley, 2003

[2] A. Diet, M. Grzeskowiak, Y. Le Bihan, M. Biancheri-Astier, M. Lahrar, C. Conessa, M. Benamara, G. Lissorgues, F. Alves, "Improvement of RFID HF tags detection with a distributed diameter coil", *Antennas and Wireless Propagation Letters*, doi: 10.1109/LAWP.2016.2544540

[3] M.Benamara, M.Grzeskowiak, A.Diet, G.Lissorgues, C.Conessa, S.Protat, Y. Le Bihan, "Twisted Loop Antenna for HF RFID detection surface'", *EuCAP,* 2016, pp. 1-5, doi: 10.1109/EuCAP.2016.7481810

[4] M. Grzeskowiak, A. Diet, M. Benamara, S.Protat, C. Conessa, M. Biancheri-Astier, F. Alves, Y. Le Bihan, G. Lissorgues, "Coaxially Distributed Diameter sub-Coil Twisted Loop Antenna in HF RFID", EuCAP, March 2017

[5] http://www.esrf.eu/Accelerators/Groups/InsertionDevices/Software/Radia

[6] http://www.ansys.com/Products/Simulation+Technology/Electronics/Signal+Integrity/ANSYS+HFSS

[7] A.Diet; C.Conessa; Y.Le Bihan; F.Alves; M.Grzeskowiak; M.Benamara; G.Lissorgues, "LF RFID Chequered Loop Antenna for pebble detection and area localization", 2016, IEEE European Microwave Week (EMC)

[8] S.Mirbozorgi, H.Bahrami, M.Sawan,B.Gosselin , "A Smart Cage With Uniform Wireless Power Distribution in 3D for Enabling Long-Term Experiments With Freely Moving Animals", IEEE Transactions on Biomedical Circuits and Systems , 2016, 10, (2), pp 424 - 434

[9] A.Diet, C.Conessa, Y.Le Bihan, et al, "Detection tube for small HF RFID tags, based on mutual coupling with a coil resonator", IEEE European Microwave Week (EMC), 2015, pp.375- 378

[10] Ib technology application note for 13,56 MHZ RFID reader antenna design http://www.ibtechnology.co.uk/pdf/antenna_1356.PDF